APTES modified SBA15 and meso-macro silica materials for the immobilization of aminoacylases from Streptomyces ambofaciens

Mohamed Chafik Bourkaib, Pierrick Gaudin, François Vibert, Yann Guiavarc'H, Stephane Delaunay, Xavier Framboisier, Catherine Humeau, Isabelle Chevalot, Jean-Luc Blin

Version of Record: https://www.sciencedirect.com/science/article/pii/S1387181121003528
Manuscript_d989d46f690a6980c554fb7f7e79c072

APTES modified SBA15 and meso-macro silica materials for the immobilization of aminoacylases from *Streptomyces ambofaciens*

Mohamed Chafik Bourkaib[a], Pierrick Gaudin[b], François Vibert[b], Yann Guiavarc'h[a], Stephane Delaunay[a], Xavier Framboisier[a], Catherine Humeau[a], Isabelle Chevalot[a*], Jean-Luc Blin[b]*

[a] : LRGP, UMR 7274 CNRS-Université de Lorraine, 2 avenue de la Forêt de Haye, TSA 40602, F-54518, VANDŒUVRE CEDEX, France

[b] : Université de Lorraine/CNRS, L2CM, UMR7565, 54500 Vandoeuvre-lès-Nancy, France

Abstract:

Aminoacylases from a crude extract from *Streptomyces ambofaciens* were described as attractive way for the synthesis of amino acids biobased surfactants. The aim of this study is to investigate the influence of the porosity and the APTES functionalization of the silica support on the immobilization and the activities of these aminoacylases. To reach this goal, a mesoporous (SBA-15) and of meso-macroporous (MMS) silica material without and with functionalization with APTES were used. The results show that the use of non-functionalized supports led to a poor enzyme loading due to electrostatic repulsion between the enzyme and the silica support. The APTES functionalization of the silica materials allow a better enzyme loading by favouring enzyme-support interactions with an increase of the immobilization rate by increasing the APTES functionalization rate from 0 to 10% especially when using MMS. However, the measurement of the catalytic performances of the enzymes immobilized on the materials shows a significant improvement of the conversion rate by increasing the APTES percentage in the case of SBA-15 unlike the enzymes immobilized on the functionalized MMS. This behaviour can be explained by the better substrate accessibility to the enzyme immobilized on the SBA-15-based materials which is mainly located on the external surface

area of the functionalized materials. The cross linking of the aminoacylases by using glutaraldehyde led to a loss of the activity due to enzyme inactivation. The LC-MS-MS analysis of the product of lysine acylation reaction shows that the regioselectivity of the enzymes after immobilization is not modified.

Keywords: aminoacylases, SBA15, mesomacroporous material, APTES functionalization, physical adsorption

1. Introduction:

Acylation reactions are largely used at industrial scale for the synthesis of food, pharmaceutics and cosmetic ingredients from natural resources [1]. Among them, bio-based surfactants, more especially amino acids surfactants (AAS), are ones of the most attractive due to their eco-compatibility, good techno-functional properties and, for some of them, attractive bioactivities which makes them molecules of choice for several industries. However, these molecules are industrially produced by chemical synthesis, especially by the Schotten-Baumann chemical reaction, requiring the use of functional group protection or activation what results in the production of large quantity of effluents which need to be reprocessed in order to reduce the environmental impact [2,3]. One of the most attractive alternatives to chemical processes is the use of enzymes to perform these reactions under mild conditions and without using and generating hazardous molecules for the environment. For this reason a wild range of enzymes has been used in different industries (cosmetics, detergents, biofuels, pharmaceutics,…) [4]. Several microbial enzymes were already described as able to perform the N-acylation reaction of amino acids in water without any protection/unprotection steps and with different regio- and chemo-selectivities allowing the control of the reaction. For these reasons, the enzymatic synthesis appears to be of great interest for the development of green and sustainable processes [5–8]. However, their protein nature makes them brittle outside their natural cellular environment where it exerts such activity [9]. Indeed, the lack of long term operational stability and the difficulty to reuse the free enzyme, in addition of their high costs, reduce the economic interest of such processes and hamper the development of industrial enzymatic production methods [10,11]. Several strategies can be used to improve the stability of the enzyme. Among them, the immobilization of the enzyme on an inert solid material might lead to an improvement in the operational life and allow recycling of the enzyme [1212-14].. A large variety of materials

exhibiting different physicochemical characteristics have been developed for enzyme immobilization [15–18]. In particular, ordered mesoporous silica, especially Santa Barbara Amorphous 15 (SBA-15) support , are widely used for enzyme immobilisation due to their properties [10,17,19]. The pore size of the support is one of the most important parameters in enzyme immobilization [20-22].. The incorporation of macropores in such supports can improve the immobilization process by decreasing mass transfer limitations by acting as transport channels of the enzyme to the mesopores and the substrates to the enzyme when the reaction is carried out [23]. Indeed, these hierarchical porous material combine the advantage of macroporous structures leading to less diffusional limitations (pores bigger than 50 nm) while maintaining high specific surface areas and the ones of the mesoporous materials which exhibit more adapted pores size and high porous volumes [24–26]. There properties might significantly increase enzyme loading [21,27].

The immobilisation method and conditions can also significantly influence both the activity and the stability of the enzyme [28-36]. Because it is simple, rapid and cheap without using any functionalized material nor toxic solvents, physical immobilisation (physisorption, entrapment, and encapsulation) is of great interest for immobilized enzyme-based processes. However, due to weak attachment of the enzyme to the support, there is a high probability to have an enzymatic desorption from the latter during the catalytic reaction due to reaction conditions or through mechanical shear forces [32]. In order to overcome this scientific bottleneck, surface property modification by grafting alkylsilanes on the hydroxyl groups of the support surface was described as improving the immobilization performances [33].. Indeed, The grafting of organosilane, like 3-aminopropyl-tri-ethoxysilane (APTES) and 3-aminopropyl-dimethyl-ethoxysilane (APDMES), on the support might change the electrostatic equilibrium and introduce other kind of low interactions such as hydrogen and hydrophobic interactions which might improve the immobilization rate [37]. Zhao *et al.* [38] immobilized

penicillin acylase (PA) on SBA-15 functionalized with different organosilanes. They demonstrated that the surface functionalization allowed higher adsorption of the enzyme due to an increase of the surface hydrophobicity and a decrease of the electrostatic repulsions. They also showed that APTES was the most suitable grafting agent for enzymatic activity compared to other organosilanes [38]. Indeed, the material surface hydrophobicity clearly influences the immobilization process and the activity of the immobilized enzyme. However, a highly hydrophobic surface can lead to a significant decrease of the enzyme activity by affecting the structural conformation of the latter. Many authors investigated the influence of the support characteristics on the structural configuration of the enzymes [35,36,39–43].

For instance, Jesionowski *et al.* [37] immobilized the acylase I from *Aspergillus melleus* on APTES functionalized and non-functionalized Stöber silica. They showed the efficiency of the APTES functionalization of the silica support where the enzyme retains 62 % of its activity compared to non-functionalized (42 %). They suggested that APTES improved the immobilization and the activity by increasing hydrogen and hydrophobic interactions.

The acylation of amino acids with fatty acids using immobilized enzyme has been already described by different authors using lipases or proteases in non-aqueous media; however the use of immobilized acylases for this reaction was rarely described [32,44,45]. In a recent work, the exceptional ability of the aminoacylases from *Streptomyces ambofaciens* to perform the reaction of N-acylation of the amino acids on their alpha amino group was described in the perspective of green synthesis of amino acids based surfactants [46]. However, these aminoacylases present low thermal stability in their free form, suggesting the possible benefit of their immobilization. Dettori *et al.* [32] immobilized these enzymes by physical and chemical methods using glutaraldehyde and glycidyle functionalization on SBA-15 and they demonstrated that the covalently immobilized enzymes lost almost all their activity (around 5% relative activity was kept) unlike the physically immobilized enzymes (around 23%

relative activity was preserved). However, by recycling the enzyme immobilized on SBA-15, a significant leaching of the adsorbed protein was observed due to the weak interactions with the support.

Given that the immobilization and the reaction processes are strongly dependent on both the porous structure (enzyme diffusion during the immobilization step) and the surface hydrophilic/hydrophilic (enzyme-support interactions) of the support, the present work aims to investigate the influence of the porosity of two silica supports and of their functionalization by 3-aminopropyl-tri-ethoxysilane (APTES) on the immobilization and activities of the aminoacylases from *S. ambofaciens.* Two porous silica supports were considered: a mesoporous (SBA-15) and a meso-macroporous (MMS) silica material. In order to tune their surface hydrophobicity [47], the grafting rate of APTES on both silicas supports was varied from 0% to 50% mol.%. The enzyme immobilization step and activity performances of the resulting material were investigated for both mesoporous SBA-15 and meso-macroporous (MMS) silica, with and without APTES functionalization.

2. Experimental

Pluronic P123 triblock copolymer, $(EO)_{20}(PO)_{70}(EO)_{20}$ and (3-aminopropyl)triethoxysilane (APTES), 98%, were purchased from Sigma-Aldrich. Tetra-methoxy-silane (TMOS), 98%, was bought from Alfa Aesar. All chemicals were used as received without further purification. Lysine (K) and lauric acid (C12) were purchased from Sigma-Aldrich, K with 99% of purity were acquired from Bachem. Aminoacylases were produced from *S. ambofaciens*.

2.1. Aminoacylases of S. ambofaciens production

The aminoacylases from *S. ambofaciens* were produced and partially purified following the procedure described by Bourkaib *et al.* (2020) and by using the same components [46].

2.2. Support preparation

2.2.1. SBA-15 preparation:

The synthesis of SBA-15 silica was carried out following the standard procedure [48]. The synthesis was conducted by dissolving 2.66 g of Pluronic 123 (P123) in 100 mL of a chlorhydric acid solution (1 M) at room temperature. After complete dissolution of P123, 4.17 g of tetramethyl orthosilicate (TMOS) were added and the mixture was kept under stirring at room temperature during 30 min. Afterwards, the solution was transferred in a Teflon-lined autoclave heated at 40°C during 24 h. Then the temperature was raised up to 100°C for 24 h. The mixture was then filtered and the material was submitted to extraction by ethanol during 48 h using a Soxhlet, in order to remove the surfactant. The obtained mesostructured silica material was finally dried at ambient atmosphere during one night to recover SBA-15 as a white powder.

2.2.2. Meso-macroprorous silica material preparation:

Hierarchical meso-macroporous silica material was prepared by "Dual Templating", combining emulsions (for the macropores) and micellar solution (for the mesopores), following a procedure reported by Blin et al. [49]. The emulsions were prepared by dissolving 760 mg of $R_8^F(EO)_9$ and 1760 mg of $R_7^F(EO)_7$ fluorinated surfactants in 7.5 g of aqueous HCl at pH = 0 at 40°C. After complete dissolution of the fluorinated surfactants, 2 g of perfluorodecalin were added to the solution under vigorous stirring. The solution was kept under stirring for 1 night. Afterwards, 980 mg of TMOS were added to the solution which was kept under stirring at 40°C for 1 h. Then the mixture was transferred in a Teflon-lined autoclave in an oven at 100°C for 24 h. Afterwards, the surfactant was removed by ethanol extraction for 48 h (soxhlet) and the resulting white powder was dried at ambient atmosphere for 24 h.

2.2.3. APTES functionalization of the materials:

Both materials were functionalized with amino-propyl-tri-ethoxy-silane (APTES) at different molar percentages allowing to cover the silicas surface with amine function. During the functionalization a covalent bonding between silanols of the silica surface and the tri-alkoxy-silane moieties of APTES is formed [32]. In order to study the effect of APTES concentration on the performance of the immobilization and the enzymatic activity, six different functionalization loadings of organic functions (APTES) in the silica were considered: 0%, 1%, 5%, 10%, 25% and 50% (functionalization loading = (moles of organosilane/moles of organosilane + moles of silica) x 100). The functionalization was conducted by adding 1 g of the silica support (SBA-15 or MMS) in toluene (50 mL). The mixture was stirred and heated at 110°C, then the required amount of APTES (table 1) was added and the suspension was kept under stirring (400 rpm) over-night under reflux. After cooling, the mixture was filtered and washed two times with toluene, followed by two times with ethanol and dried over-night under vacuum to recover the functionalized material as a powder. The resulting functionalized supports are labelled as $SBA15^{n\%}$ for functionalized SBA-15 and $MMS^{n\%}$ for functionalized meso-macroporous support, where n represent the silica/organic group molar ratio.

Table 1:

2.3. Immobilization of the aminoacylases of *S. ambofaciens* on the different materials

The physical adsorption of the aminoacylases from *S. ambofaciens* was conducted by suspending 200 mg of the support (without or with functionalization) in 36 mL of TRIS buffer (TRIS 25 mM in water, NaCl 50 mM, pH=8) and 1 mL of the aminoacylases solution (20 mg/ mL) was then added. The mixture was stirred during 18 h at 4°C. The final mixture was

filtered, washed two times with TRIS buffer and dried one night under air to afford functionalized or non-functionalized SBA-15-acylase or MMS-acylase.

Cross liking enzyme aggregates (CLEAs) of the immobilized enzyme on the functionalized SBA-15 with 50% APTES: the immobilized acylases on the SBA-15 functionalized with 50% APTES was conducted using different molar percentages of Glutaraldehyde from Sigma Aldrich with 25% purity. The addition of Glutaraldehyde results in a covalent bridge between the amino acids residues of the enzymes which can improve the catalytic performance and the stability of the enzyme [49]. In order to study the effect of glutaraldehyde concentration, different molar percentages were used: 0%, 1%, 5% and 10% (glutaraldehyde rate = (moles of glutaraldehyde x 100 / (moles of glutaraldehyde + moles of silica)). The functionalization was conducted by mixing 0.5 g of the functionalized SBA-15 in 5 mL of Tris HCl 25 mM, NaCl 50 mM, pH 8 containing the appropriate quantity of glutaraldehyde (34, 175 and 370 µL of glutaraldehyde solution for the 1, 5 and 10% molar ratio, respectively). The mixture was stirred at 4°C and 100 rpm by rotatory agitation overnight. The mixture was then filtered and washed two times with the Tris HCl buffer and dried one night under vacuum to recover the final material as a brick red powder proofing the glutaraldehyde incorporation and CLEAs formation. As a reference sample, the free enzyme was also treated in the same way by using 370 µL of glutaraldehyde.

2.4. Characterization of the materials

Nitrogen adsorption–desorption isotherms, Small angle X-ray scattering (SAXS) experiments and solid-state NMR spectra were all conducted following the same methodology and machinery described by [32]

Macropores were detected using mercury porosimetry on a Micromeritics Autopore IV 9500. The penetrometer (stem volume = 0.412 ml, penetrometer volume = 1ml) was filled with 0.1

g of the sample. A low pressure (0.1 to 15 psia) followed by a high-pressure analysis (15 to 60 000 psia) were performed in order to detect pores down to 5 nm in diameter, the equilibration time is 10 seconds.

2.5. Enzyme activity assays

2.5.1. Hydrolysis reaction

After the adsorption process, the activity of all immobilized enzyme was evaluated for their hydrolytic activity of the Nα-acetyl-L-lysine as substrate. The enzymatic hydrolysis was carried out in test tubes containing 1.8 mL Tris-HCl (25 mM) NaCl (50 mM) at pH 8, 0.2 mL of the substrate (40 mM) and the quantity equivalent to 1 mg/mL of immobilized enzyme or the free enzyme (around 0.5 mg/mL) for a 2 mL final volume. The reaction was performed during 24 h at 37°C and 500 rpm stirring. Samples of 100 µL were withdrawn and diluted 10 times in water for TLC and HPLC-MS analyses. The conversion rate was calculated from the measurement of lysine concentration released during the hydrolysis and corresponding to the percentage of lysine produced from acetyl-lysine hydrolysis by free or immobilized enzymes. For recycling experiments, activity of immobilized aminoacylase was determined after 3 cycles and the corresponding relative hydrolytic activity of the immobilized enzymes was determined by taking the first reaction as reference (set as 100%). The specific activity of the enzymes was defined as the amount of lysine produced reported to the quantity (mg) of aminoacylases in the reaction medium.

2.5.2. Acylation reaction

The N-α-lauroyl-lysine synthesis activity of the aminoacylases was carried out in test tubes containing 0.1 M of lysine and 0.1 M of lauric acid in 2 mL of Tris-HCl (25 mM), NaCl (50 mM) at pH 8. A quantity equivalent to 1 mg/ml of the immobilized protein or 0.5 mg/mL of

the free enzyme was then added to start the reaction. The reaction was conducted during 48 h at 45°C and 250 rpm stirring. 100 µL samples were withdrawn and diluted 10 times with methanol/water (80/20, v/v) solution for the evaluation of the synthetic activity by TLC and HPLC.

2.5.3. Analysis of the reaction medium

2.5.3.1. Qualitative analysis by TLC

Before HPLC analysis, qualitative analysis of the production of lysine from the hydrolysis reaction and the acylated product from synthesis reaction were evaluated by TLC on Kieselgel G 60 Plates 20 cm×20 cm (Merck, Darmstadt, Germany). The mixture butanol (60 %)/acetic acid (20 %)/water (20 %) was used as mobile phase. Knowing that lysine contains two amino groups allowed the detection by spraying a commercial solution of ninhydrin reagent (Sigma-Aldrich).

2.5.3.2. Quantitative analysis by HPLC

Quantitative analysis of the lysine produced during the hydrolysis reaction was performed by high-pressure liquid chromatography (HPLC) coupled with a mass spectrometry (MS) Shimadzu®. The separation of the lysine from the other constituents was carried out using Hypercarb column (100 x 2,1 mm ; 5µm ; Phenomenex, USA). During the analysis the column temperature was set to 10°C. The mobile phases was composed of ultrapure water containing 20 mM Nonafluoropentanoic acid (NFPA) for phase A and pure acetonitrile for phase B. the phase B gradient used for the analysis was : 0 to 15 % during 10 min then 15 to 26% during 10 min then 26 to 50% during 10 min followed by an isocratic gradient at 50% during 10 min before the decrease of the concentration to 0% phase B for the equilibration of the column. The detection and the quantification of the lysine was done using mass analysis

data lysine transition from M+H/z=147.10 uma major ion daughter at M+H/z=84.10 uma, coming from the dissociation generated after the collision with argon, in MRM positive mode (Multiple Reaction Monitoring). The apparatus is equipped with double ionisation or DUIS (Dual Interface Ionization System) with the ElectroSpray Ionization (ESI) and Atmospheric Pressure Chemical Ionization (APCI).

For synthesis production of lauroyl-lysine, the quantification of reaction conversion yield was conducted using HPLC (LC10 AD-VP, Shimadzu, France) equipped with a UV detector at 214 nm and a light-scattering low temperature evaporative detector (Shimadzu, France). A C18 amide 125×2.1 mm (Altima®, Altech, France) maintained at 25°C was used as the suitable separation column. The mobile phase (0.2 mL/min flow rate) consisted of solvent A: methanol/water/TFA (60/40/0.1 v/v/v) and solvent B: methanol/TFA (100/0.07). A linear elution gradient was applied to reach 95 % methanol/TFA after 6 min. This methanol concentration was maintained for 13 min and then decreased in 1 min to reach the initial methanol/water ratio until the end of the run (35 min). Calibrations were performed using standard curve fatty acids and purified commercial α-lauroyl-lysine. The substrate conversion yield was determined using the following equation: conversion yield (%) = (1 - ([fatty acid]$_{mol/L}$ consumed / [fatty acid]$_{mol/L}$ initial) × 100.

3. Results and discussion

3.1. Immobilization of acylases onto the bare porous silica and activity of the supported biocatalyts

To investigate the influence of the porosity on the amount of immobilized enzyme and on its activity, the bare SBA-15 and MMS silicas was first used as support. The SBA-15 mesostructured silica adsorption/desorption isotherms exhibit a type IV isotherms, characteristic of the presence of mesopores in the materials according to the IUPAC

classification (Fig 1A) [50]. A H1 hysteresis loop with two parallel and vertical branches, which are assigned to well defined cylindrical mesopores with homogeneous size is observed. The physisorption isotherm of the MMS material is a combination of type IV and type II isotherms, featuring the presence of both meso- and macro-pores. The BJH mesopore size distribution represented in 1 B show a sharp peak in the case of SBA-15 while MMS shows a broader mesopore size distribution, evidencing a better homogeneity of the mesopore size for the SBA-15 material.

The values of the BET specific surface areas (S_{BET}), the porous volumes (V_{por}) and the pore diameter ($\varnothing_{pore}$) are reported in table 2. Both materials exhibit nearly similar mesopores diameter (7.8 nm for MMS and 8.7 nm for SBA-15). However, the presence of macropores in the MMS silica results in higher porous volume (1.7 cm^3/g) and specific surface area (802 m^2/g) compared to SBA-15 (0.82 cm^3/g and 650 m^2/g, respectively). Such characteristics are expected to allow the immobilization of higher amount of enzyme on the MMS support. The mercury porosity analysis (Figure 2) features the presence of macropores whose macropore size distribution is centred on 4.7 µm. In accordance with mercury porosity characterization, micrographs obtained by scanning electron microscopy (Fig 2) show the presence of sponge-like silica particles with macropores having a size in the range from 1 to 3 µm.

The SAXS patterns of SBA-15 shows three reflection peaks at q1=11.0 nm^{-1}, q2=6.3 nm^{-1} and q3=5.0 nm^{-1} which verify the relation q1:q2:q3 = 1: √3: 2 and were assigned respectively to the (10), (11) and (20) diffraction planes of the 2D hexagonal arrangement of the mesoporous channels (Fig. 1. 1C). The first reflection peak (q1) was used to calculate the d_{10} Bragg distance which is in accordance with the literature (10.9 nm) [31,32]. The Bragg distance was used to determine the unit cell dimension ($a_0 = 2d_{10}/\sqrt{3}$ = 12.7 nm). The mesopore wall thickness was estimated to 4.0 nm by subtracting the pore size diameter,

determined by N_2 sorption isotherm to the unit cell a_0 (tab 2). In the case of MMS (Fig. 1. 2C), only one broad peak is detected at around 9.0 nm^{-1}, suggesting the formation of a wormhole-like mesopore network [49]. Assuming that the Bragg distance represents the sum of the mesopore diameter and of the mesopore wall thickness, the later can be estimated to 1.2 nm, which is 3 times lower than the one of the SBA-15.

The enzyme immobilization was carried out in the same conditions for both supports. The amount of the acylases immobilized on the supports was nearly similar with around 3 % for the SBA-15 and more than 4% for the MMS. The slightly higher enzyme loading might result from both the presence of macropores which favour the enzyme diffusion in the porous network and to the higher porous volume (V_{por}) and specific surface area (S_{BET}) compared to the SBA-15 material (table 2). For both supports, after immobilization the shape of the N_2 sorption isotherm was similar to the one of the bare silicas (Fig 1. 1A and 2A). A very important decrease of the S_{BET}, V_{por} and the pore diameter ($\varnothing_{pore}$), more pronounced when using MMS, was observed (fig 1 and tab 2). This result can be assigned to the mesopore filling with the enzyme and/or the partial alteration of the silica structure during the immobilization process performed in basic medium (pH=8). Indeed, silica is prone to hydrolysis under aqueous basic conditions. SBA-15 is less prone to such textural modifications which is attributed to its higher wall thickness an higher level of silica condensation, what limits the structure collapse [19]. Such phenomenon is confirmed by SAXS patterns which evidence no significant changes before and after adsorption of the enzyme on the SBA-15 materials. On the contrary, the diffraction peak observed at 9.0 nm^{-1} for the MMS material before immobilization nearly disappears after enzyme immobilization, suggesting a partial collapse of the mesostructure. In both cases the immobilization rate was lower than in the literature [43,32]. Considering that the acylases present a PI of around pH 7 [36,38], such a result can be explained by electrostatic repulsions between the enzyme and

the supports , which have an isoelectric point (PI) around pH 2-3 . The variation of the mesopore volume and of the specific surface area indicate adsorption of the enzyme in the mesopores, however, the adsorption of a part of the enzyme at the outer surface of the materials cannot be excluded.

Fig 1.

Fig 2.

In order to evaluate their potential recycling, the behaviour of the immobilized enzymes was evaluated along successive experiments by using the hydrolytic reaction of the α-acetyl-lysine as a reference reaction. The activity was evaluated by carrying out the reaction in 2 mL flask with magnetic stirring during 24 h. Then, the support was separated from the reaction medium by centrifugation and washed two times before being used for the next reaction (with a fresh substrate solution). The support was recycled two times (Figure 3). The first catalytic activity of the immobilized enzymes was around 100 time much lower than the one of the free enzymes. As shown in figure 3, a significant decrease of the activity but a stability of the specific activity was observed which mean that the decease of the enzymatic activity was due to protein leaching along cycles. Several authors described the same behaviour of immobilized enzymes on SBA-15 [32,52]. This can be explained by the weak interactions (van der walls or, at lower level, by hydrogen interactions) between the silica material and the protein. The higher desorption rate observed in the case of meso-macroporous support can be assigned either to the easy diffusion of the enzyme from inside the pore towards the reaction medium and/or to the collapse of the silica structure due to its low wall thickness.

Fig 3.

Table 2.

3.2. Immobilization of acylases onto APTES-functionalized mesoporous (SBA-15) and meso-macroporous silica (MMS) supports

In order to investigate the possible improvement of the activity and stability of the immobilized enzymes by the silica surface modification, both materials were functionalized with 3-aminopropyl-tri-ethoxysilane (APTES).

As reminded in the introduction, several authors investigated the use of organosilane-functionalized silica materials for the immobilization of acylases [37,38,43]. They demonstrated that APTES-functionalized materials seem to be the most suitable to improve the activity and the stability of penicillin acylase and the acylase I from *Aspergillus melleus*. For this reason, the APTES was used in this study with different loading, in order to evaluate the influence of the surface modification. The grafting of APTES changes the surface properties of the silica by increasing surface hydrophobicity due to the presence of propyl groups and by reducing the quantity of free hydroxyl groups [43]. Moreover, the nature of the interactions between the enzyme and the functionalized support strongly depend on their respective pI and of the pH. Electrostatic interactions between the positively charged amino group of APTES ($R\text{-}NH_3^+$) and the negatively charged carboxyl group of the glutamic and aspartic acid residue of the surface of the immobilized proteins possibly occur but due to the lack of information about the 3D structure of the enzyme, there is no way to confirm this hypothesis. It is also possible to observe an improvement of the hydrogen interactions between non-protonated APTES amino group ($R\text{-}NH_2$) and the enzyme as described in the literature [37]. The functionalized materials (SBA-15 and MMS) were characterized before and after immobilization of the aminoacylases of *S. ambofaciens* and the activities of the immobilized enzymes were compared. Silicium NMR (^{29}Si NMR) was used to characterize the functionalization rate of the supports. The ^{29}Si NMR spectra of the functionalized SBA-15 and MMS (with 1% and 50% APTES) are given in fig.4a. Before functionalization, the ^{29}Si

RMN spectrum features the presence of Q2 ($Si(OSiOH)_2$), Q3 ($Si(OSi)_3OH$) and Q4 ($Si(OSi)_4$ species assigned to the peaks at -95 ppm, -105 ppm and -115 ppm. After grafting with 1% APTES, Q3 and Q4 species are still observed and a weak peak appears at -71 ppm, assigned to T3 ($(SiO)_3SiC$) species, evidencing the covalent linking of the propylamine moieties to the silica support. At higher loading (50% APTES) the T3 peak becomes more intense and a second peak at -64 ppm appears, assigned to T2 ($(SiO)_2Si(OH)C$) species, both peaks featuring the higher grafting rate of APTES on silica material as compared to the 1% APTES material.

By integration of the Tn and Qn signals, using the formula $\int Tn/(\int Tn + \int Qn)$, the functionalization rate of the silica support by APTES was estimated. Results are reported in Table 3. Noteworthy, the ^{29}Si RMN spectra of the APTES-functionalized materials are similar before and after enzyme immobilization, suggesting that the immobilization procedure does not impact (or in a minor extent) the covalent bonds between APTES and silica.

Table 3:

Carbon NMR (^{13}C CPMAS NMR) spectra of the supports functionalized with 1% and 50% APTES before acylase immobilization are presented in fig. 4b. Three major peaks are observed for SBA-15 at around 43, 23 and 10 ppm and at around 39, 26 and 6.5 ppm for MMS with APTES (50%). These peaks correspond to the carbon atoms of the CH_3-N, CH_2 and CH_3-Si groups of APTES, respectively [32,37,53].

After enzymes immobilization, a new peak appears at around 174 ppm, for the SBA-15 functionalized with 50% APTES. This signal might be the result of the peptide linkage (NH-CO). Another peak is present at around 60 ppm, especially when the enzymes were immobilized on SBA-15, it might correspond to the carbon atoms close to a nitrogen atom of the α-amino group of the amino acids chain (NH-CH(R)-CO) [31]. Those peaks confirm the

presence of the enzyme at the surface of the materials however the low protein immobilized amount make the detection by NMR difficult.

SAXS patterns reported on fig. 5 A and B show that the mesostructure of the materials is preserved after the grafting step. Indeed, the reflexion spectra of the functionalized and non-functionalized SBA-15-based materials are similar, with the presence of three reflection peaks characteristics of the hexagonal arrangement of the mesopores, as discussed above. Similarly, MMS-based materials exhibit similar SAXS patterns before and after the functionalization. After immobilization of acylases on the different supports, the same trend was observed as the one described above, i.e.: no significant change in the ordered hexagonal mesopores of the SBA-15 is noticed while a partial collapse of the mesoporous structure (decrease of the peak intensity) of the MMS is observed.

After the functionalization, the general shape of the adsorption isotherms is not modified (fig 5. C and D). However, it is evident that higher the APTES content, lower the porous volume of the materials which is assigned to pore filling by the grafted organic moieties. Regarding the SBA-15-based materials, a significant decrease of the BET specific surface area, porous volume and mesopore diameter after enzymes immobilisation is observed on the non-functionalized SBA-15 support (fig 6). Such a result can be attributed to the supplementary mesopore filling by the enzymes. However, it is noteworthy that no significant change of the porous volume and mesopore diameter is observed after enzymes immobilization on the APTES-functionalized SBA-15-based materials. This might be due to the presence of grafted aminopropyl groups that prevent the diffusion of the enzymes toward the inside of the mesoporous network. The slight decrease of the BET specific surface area after enzymes immobilization on the APTES-functionalized SBA-15-based materials can be assigned to the enzyme adsorption on the external surface area of the support. Contrarily to SBA-15-based materials, a strong decrease of the mesopore diameter is observed for the MMS-based

materials after enzymes immobilization. Such a result can be assigned to the pores filling by the enzyme and/or the partial collapse of the silica structure along the immobilization step, as discussed previously for the non-functionalized support.

Fig 4.

Fig 5.

Fig 6.

After the adsorption of the aminoacylases from *S. ambofaciens* on the different kind of functionalized materials, the quantity of immobilized proteins was determined by BCA analysis of the filtrate, and the washing solution. As shown in figure 7, the quantity of the adsorbed proteins depends on the nature of the support and on the functionalization rate. The enzyme loading on MMS is more or less 1.5 time higher than on SBA-15. This result can be related to the presence of the second pore network; i.e. the macropore one in the MMS material which improves the accessibility of the enzyme into the porous network. The results show that the functionalization rate considerably improves the immobilized acylases amount (more than 2 times) for both porous materials when increasing the APTES loading from 0 to 10%. For APTES loading higher than 10% and up to 50% the enzyme loading reaches a plateau at around 0.65 mg prot/mg material for SBA-15-APTES support and around 0.95 mg prot./mg material for MMS-APTES material. The increase of enzyme loading for APTES grafting from 0% to 10% can be explained by the modification of surface properties of the materials by grafting APTES molecules which reduce the presence of hydroxyl group and increase the possible hydrophobic, electrostatic and hydrogen interactions between the grafted organosilane and the enzyme. The reduction of the presence of the free -OH at the surface might prevent the electrostatic repulsion caused by the negative charge of the material and the enzyme surface at the pH used during the immobilization process (pH 8 > pI of the material

and the enzymes). Moreover, the hydrophobic interactions between the propyl part of the APTES and the amino acids residues of the enzyme surface might be promoted. The same trend was described by Chong *et al.* [38]. The authors reported a faster and better enzyme immobilization of penicillin acylase on SBA-15 functionalized with APTES, compared to the native SBA-15. They also described an immobilization of the penicillin acylase on the external surface of the SBA-15 containing pore size smaller than the enzyme diameter unlike the support with larger pore size [38]. For both supports, the stabilization of the immobilization rate after 10% APTES functionalization can be attributed to a saturation of the surface of the materials by the APTES and a possible obstruction of the mesopores by organic moieties.

Fig 7.

The results concerning the acylases immobilization show a very important difference between SBA-15 and MMS supports. In the case of the functionalized SBA-15, whatever the functionalization rate, only very slight changes of the specific surface area and of the pore volume are observed. This can be related to diffusional limitations of the enzyme into the mesopores. Indeed, as shown in figure 6. C, no change in the mesopore diameter was observed after immobilization on the functionalized unlike the non-functionalized SBA-15. The quantification of the protein immobilized on the support (fig 7) shows an improvement of the adsorbed amount of enzymes by increasing the APTES rate and the ^{13}C CPMAS NMR spectra confirm clearly the presence of the enzymes at the surface of the functionalized materials. Those observations suggest that a major part of the enzyme is immobilized on the external surface area of the functionalized SBA-15 assigned to diffusional limitations of the enzymes into pores of the SBA-15, due to the presence of APTES.

The MMS-based materials show a completely different behaviour after the immobilization on the functionalized material. An important decrease of the specific surface area and of the

porous volume is observed after immobilization on the different functionalized MMS. The final values reached are similar to the ones of SBA-15 materials after immobilization. These results strongly suggest that the immobilization of the acylases occurred inside the pores of the MMS, promoted by the presence of larger pore diameter and the possible funnel organization between macropores and mesopores allowing a better diffusion of enzyme molecules inside the mesoporous structure. Indeed, according to the figure 6. C an important decrease of the pore size and an increase of the wall thickness of the mesopores was registered, confirming the immobilization of the acylases inside the pores. However, the possible immobilization of the enzymes at the external surface cannot be completely excluded. In order to check if there were a collapse of the MMS mesoporous structure causing a decrease of the material properties, the SBA-15 and MMS functionalized with 5% and 50% functionalized was treated with the buffer (buffer Tris-HCl 25 mM, NaCl 50 mM, pH 8) in the same way as when the immobilization was conducted. The adsorption/desorption isotherm showed a significant decrease (50%) of the porous volume of the MMS compared to the SBA-15 where no change was registered after the treatment with only the buffer (figure 6.D). In addition, the pore size of the material after the treatment without enzyme showed also a significant decrease passing from 6.8 to 4.6 for MMS functionalized with 5% APTES and from 5.2 to 4.9 for the one functionalized with 50% APTES while no change of the mesoporosity of the SBA-15 were observed. This result confirms the collapse of the mesostructured of the MMS material due to a pore wall thicknesses lower than the one of the SBA-15 allowing more resistance (pore wall thicknesses of 2.5 nm for MMS and around 4 nm for SBA-15). The reduction of the mesopore size may cause a diffusional limitation of the enzymes into the mesopores which mean that the they are essentially immobilized in the macro-porosity of the MMS. On the other hand, if the enzymes enter the mesopores which is likely the case because of the higher decrease of the pore size when the enzyme solution is

used, they can be entrapped in there which can stabilise the enzyme inside the pore but can induce a diffusional limitation of the substrate to the enzyme during the reaction. This can be confirmed by the activity evaluation.

3.3. Activity of the physically immobilized aminoacylases on APTES-functionalized materials (SBA-15 and MMS)

In order to evaluate the catalytic performances of the immobilized enzymes on the different functionalized materials, the N-α-acetyl-L-lysine hydrolysis reaction was performed in Tris HCl buffer at pH 8 and with the same enzyme equivalent amount (1 mg proteins/mL). The conversion rates of the immobilized enzymes are presented on figure 8.A. The results show that the immobilized enzymes exhibit a catalytic activity, what can be explained by the orientation of the enzyme at the surface of the support by exposing the active site to the reaction medium resulting in an increase of the enzyme/substrate interactions and a better diffusion of the reactants towards the active sites. However, as expected, in all cases the hydrolytic activity was much lower than the free enzymes which show a complete hydrolysis of the substrate after 24 h in the same operational conditions. Several authors described an improvement of the catalytic activity after immobilization of acylases on APTES functionalized materials. Chong *et al.* [38] immobilized the penicillin acylase on functionalized and non-functionalized SBA-15. They showed that the APTES was the most appropriate organosilane compared to other organosilanes (4-(trimethoxysilyl)-butyronitrile vinyltriethoxysilane, (3-Mercaptopropyl)tri-methoxysilane, …) for the immobilization of this enzyme with around two times improvement of the activity compared to the one immobilized on non-functionalized SBA-15 [38]. Jesionoxski *et al.* [37] performed the immobilization of the acylase I from *Aspergillus melleus* on amino and carbonyl functionalized Stöber silica. They also demonstrated an important increase in the catalytic activity by using APTES functionalized materials. This was related to a better orientation of the enzyme avoiding the

obstruction of the active site of the enzyme. Radhakrishna *et al.* (2013) explained the phenomena implicated in the improvement of the catalytic activity of the enzymes immobilized on moderately hydrophobic surface by a better stiffening of the enzyme at the surface of the material without any conformational disruption [41].

Regarding our results (figure 8.A), the catalytic activity of the SBA-15-APTES-Enzyme materials seems to be correlated to their enzyme loading, which itself depends on the APTES functionalization rate of the support, as discussed above. An increase of the enzyme loading and material activity is observed for APTES grafting rate increasing from 1% to 10%, then a plateau is reached between 10% and 50%. The MMS-based materials exhibit a significantly lower activity than the SBA-15-based ones, although the enzyme loading is around 1.5 times higher on the MMS support as compared to the SBA-15 one. Such results feature that the enzyme activity is much higher on the SBA-15 supports than one the MMS ones. Moreover, the activity of the immobilized enzymes on the functionalized MMS is weakly affected by the APTES rate unlike the functionalized SBA-15. These results can be related to the partial collapse of the MMS porous network observed in the previous section, restricting the accessibility of the substrate to the enzyme. On the contrary, in the case of APTES functionalized SBA-15 the support characterisations strongly suggest that the main part of the enzymes is adsorbed at the external surface of the material which makes them more exposed to the substrate, thus reducing the diffusional limitations of the substrate to the active site. Also, the presence of APTES at the surface of the support can change the orientation of the immobilized enzyme leading to a better exposition of the active site to the substrats. The thicker walls of SBA-15 make it more resistant to collapsing phenomena compared to MMS. Based on these results, the functionalized SBA-15 was selected for the rest of the study.

The ability to reuse the immobilized biocatalyst is an important factor to determine the economic viability of a process. The immobilization of the acylases on non-functionalized

SBA-15 previously described, showed an important leaching of the enzymes after the first use. The functionalization of the SBA-15 with APTES is supposed to improve the stabilization of the enzymes on the material by introducing hydrophobic interactions and avoiding electrostatic repulsions. The results of the measurement of the protein desorption after several uses of the supported material is presented on figure 8.B. The immobilized enzymes on the functionalized material present a better stability after the first reuse compared to the non-functionalized one. However, after the second reuse, an important leaching of the protein was observed to reach the same amount of enzymes as the one with non-functionalized material. The desorption of the enzymes can be explained by the moderately hydrophobic surface which exhibit better affinity for this enzyme than the highly hydrophilic one of pure SBA-15 but not enough to retain the enzymes and to resist to the mechanical shear of the magnetic agitation mode used during the reaction.

These immobilized enzymes were also evaluated for their synthetic activity by using lauroyl-lysine synthetic reaction, using L-lysine and lauric acid as substrates with an equimolar ratio. The relative activity compared to the activity of the free enzymes is presented on the figure 8.C. The evolution of the synthetic activity depending on the APTES functionalization rate follows the same trend as the one obtained for the hydrolytic activity: an increase of the APTES rate results in an increase in the conversion rate. In order to check if there was no change in the regioselectivity of the immobilized acylases, LC-MS-MS analysis of the reaction products was conducted. In all cases, the results show the apparition of only a mono-acylated product corresponding to the acylated lysine on the alpha amino group. The same MS^2 profile was obtained by using the free enzymes [46]. However, in all cases, a significant loss of the synthesis activity (more than 90 %) was observed compared to the free acylases. This loss can be explained by diffusional limitations of the substrate emulsion to the active site which was more difficult than the use of a single molecule as substrate. The evaluation of

the protein leaching after the three days synthesis reaction shows that around 23 % was desorbed from the silica materials.

In order to reinforce the stability of the enzymes at the surface of the immobilization support, an additional chemical treatment of the immobilized enzymes on the SBA-$15^{50\%}$ with glutaraldehyde was conducted. This treatment allows the formation of cross-linking enzyme aggregates (CLEAs) between the immobilized enzymes on the material. Different glutaraldehyde ratios were used in order to determine its influence on the activity. After the treatment, no loss of the already immobilized enzymes was detected by BCA analysis of the filtration and washing solutions. According to the results reported on the figure 8.D the formation of cross-linking between the enzymes led to a dramatic loss of the activity compared to the non-treated material. The increase of the glutaraldehyde percentage was accompanied with a decrease of the enzymatic activity. The SAXS analysis didn't show any structural modifications of the mesopores. The production of CLEAs using the free enzymes and 10% glutaraldehyde showed a complete loss of the catalytic activity. This result can be explained by the formation of covalent bridges between the protein amino acids residues causing a distortion of the protein conformation and the active site. Due to the fragile structure of those aminoacylases, the CLEAs formation was not suitable for the improvement of both the activity and the stability of these enzymes.

Fig 8.

4. Conclusion:

The aim of this study was to investigate the influence of the pores size and of the surface functionalization of (macro)-mesoporous silica-based materials on the immobilization and the activity of the aminoacylases from *S. ambofaciens*. The use of meso-macroporous materials (MMS) allowed higher physisorption of the enzymes due to the presence of macropores but

the activity was better after immobilization on mesoporous silica material (SBA-15). The functionalization of the materials with APTES allowed an increase of the catalytic performances of the enzymes related to a better orientation of the active site influenced by the increase of the surface hydrophobicity. However, the stability was low even after the surface functionalization. Furthermore, it was demonstrated that the aminoacylases from *S. ambofaciens* are cobalt dependent: work is in progress to favour the co-condensation of cobalt in the material preparation that might also improve the catalytic performances.

Acknowledgments:

This work was mainly supported by the French National Research Agency (ANR) through the "ISEAPIM3" project (ANR-15-CE07-0023-01) and the "Impact biomolecules" project of the « Lorraine Université d'Excellence » (PIA-ANR).

References:

[1] C. Rondel, I. Alric, Z. Mouloungui, J.-F. Blanco, F. Silvestre, Synthesis and Properties of Lipoamino Acid–Fatty Acid Mixtures: Influence of the Amphiphilic Structure, Journal of Surfactants and Detergents. 12 (2009) 269–275. https://doi.org/10.1007/s11743-009-1121-y.

[2] R.A. Sheldon, J.M. Woodley, Role of Biocatalysis in Sustainable Chemistry, Chem. Rev. 118 (2018) 801–838. https://doi.org/10.1021/acs.chemrev.7b00203.

[3] R.A. Sheldon, D. Brady, Broadening the Scope of Biocatalysis in Sustainable Organic Synthesis, ChemSusChem. 12 (2019) 2859–2881. https://doi.org/10.1002/cssc.201900351.

[4] A. Madhavan, R. Sindhu, P. Binod, R.K. Sukumaran, A. Pandey, Strategies for design of improved biocatalysts for industrial applications, Bioresource Technology. 245 (2017) 1304–1313. https://doi.org/10.1016/j.biortech.2017.05.031.

[5] M. Koreishi, D. Zhang, H. Imanaka, K. Imamura, S. Adachi, R. Matsuno, K. Nakanishi, A Novel Acylase from Streptomyces mobaraensis that Efficiently Catalyzes Hydrolysis/Synthesis of Capsaicins as Well as N-Acyl-l-amino Acids and N-Acyl-peptides, J. Agric. Food Chem. 54 (2006) 72–78. https://doi.org/10.1021/jf052102k.

[6] M. Koreishi, R. Kawasaki, H. Imanaka, K. Imamura, K. Nakanishi, A novel ∈-lysine acylase from Streptomyces mobaraensis for synthesis of N∈-acyl-l-lysines, Journal of the American Oil Chemists' Society. 82 (2005b) 631–637. https://doi.org/10.1007/s11746-005-1121-2.

[7] L. Dettori, F. Ferrari, X. Framboisier, C. Paris, Y. Guiavarc'h, L. Hôtel, A. Aymes, P. Leblond, C. Humeau, R. Kapel, I. Chevalot, B. Aigle, S. Delaunay, An aminoacylase activity from Streptomyces ambofaciens catalyzes the acylation of lysine on α-position and peptides on N-terminal position, Engineering in Life Sciences. 18 (2017) 589–599. https://doi.org/10.1002/elsc.201700173.

[8] Y. Takakura, Y. Asano, Purification, characterization, and gene cloning of a novel aminoacylase from Burkholderia sp. strain LP5_18B that efficiently catalyzes the synthesis of N-lauroyl-l-amino acids, Bioscience, Biotechnology, and Biochemistry. 83 (2019) 1964–1973. https://doi.org/10.1080/09168451.2019.1630255.

[9] M. Bilal, J. Cui, H.M.N. Iqbal, Tailoring enzyme microenvironment: State-of-the-art strategy to fulfill the quest for efficient bio-catalysis, International Journal of Biological Macromolecules. 130 (2019) 186–196. https://doi.org/10.1016/j.ijbiomac.2019.02.141.

[10] R.A. Sheldon, S. van Pelt, Enzyme immobilisation in biocatalysis: why, what and how, Chem. Soc. Rev. 42 (2013) 6223–6235. https://doi.org/10.1039/C3CS60075K.

[11] K.C. Badgujar, B.M. Bhanage, Immobilization of lipase on biocompatible co-polymer of polyvinyl alcohol and chitosan for synthesis of laurate compounds in supercritical carbon dioxide using response surface methodology, Process Biochemistry. 50 (2015) 1224–1236. https://doi.org/10.1016/j.procbio.2015.04.019.

[12] A.S. Bommarius, M.F. Paye, Stabilizing biocatalysts, Chem. Soc. Rev. 42 (2013) 6534–6565. https://doi.org/10.1039/C3CS60137D.

[13] M. Hartmann, X. Kostrov, Immobilization of enzymes on porous silicas – benefits and challenges, Chemical Society Reviews. 42 (2013) 6277–6289. https://doi.org/10.1039/C3CS60021A.

[14] J. Zdarta, A.S. Meyer, T. Jesionowski, M. Pinelo, A General Overview of Support Materials for Enzyme Immobilization: Characteristics, Properties, Practical Utility, Catalysts. 8 (2018) 92. https://doi.org/10.3390/catal8020092.

[15] J.M. Nelson, E.G. Griffin, ADSORPTION OF INVERTASE., J. Am. Chem. Soc. 38 (1916) 1109–1115. https://doi.org/10.1021/ja02262a018.

[16] A.A. Homaei, R. Sariri, F. Vianello, R. Stevanato, Enzyme immobilization: an update, J Chem Biol. 6 (2013) 185–205. https://doi.org/10.1007/s12154-013-0102-9.

[17] B. Thangaraj, P.R. Solomon, Immobilization of Lipases – A Review. Part II: Carrier Materials, ChemBioEng Reviews. 6 (2019) 167–194. https://doi.org/10.1002/cben.201900017.

[18] M. Bilal, H.M.N. Iqbal, Chemical, physical, and biological coordination: An interplay between materials and enzymes as potential platforms for immobilization, Coordination Chemistry Reviews. 388 (2019) 1–23. https://doi.org/10.1016/j.ccr.2019.02.024.

[19] J. Jacoby, A. Pasc, C. Carteret, F. Dupire, M.J. Stébé, V. Coupard, J.L. Blin, Ordered mesoporous materials containing Mucor Miehei Lipase as biocatalyst for transesterification reaction, Process Biochemistry. 48 (2013) 831–837. https://doi.org/10.1016/j.procbio.2013.04.003.

[20] H.-X. Zhou, K.A. Dill, Stabilization of Proteins in Confined Spaces, Biochemistry. 40 (2001) 11289–11293. https://doi.org/10.1021/bi0155504.

[21] Y. Wang, F. Caruso, Mesoporous Silica Spheres as Supports for Enzyme Immobilization and Encapsulation, Chem. Mater. 17 (2005) 953–961. https://doi.org/10.1021/cm0483137.

[22] L. Bayne, R.V. Ulijn, P.J. Halling, Effect of pore size on the performance of immobilised enzymes, Chem. Soc. Rev. 42 (2013) 9000–9010. https://doi.org/10.1039/C3CS60270B.

[23] E. Santamaría, A. Maestro, M. Porras, J.M. Gutiérrez, C. González, Preparation of structured meso–macroporous silica materials: influence of composition variables on material characteristics, J Porous Mater. 21 (2014) 263–274. https://doi.org/10.1007/s10934-013-9771-6.

[24] S. Kim, J. Jacoby, M.-J. Stebe, N. Canilho, A. Pasc, Solid Lipid Nanoparticle - Functional Template of Meso-Macrostructured Silica Materials, American Chemical Society, 2015. https://hal.univ-lorraine.fr/hal-01959404 (accessed February 18, 2020).

[25] J. Esquena, J. Nestor, A. Vílchez, K. Aramaki, C. Solans, Preparation of Mesoporous/Macroporous Materials in Highly Concentrated Emulsions Based on Cubic Phases by a Single-Step Method, Langmuir. 28 (2012) 12334–12340. https://doi.org/10.1021/la302120f.

[26] J. Nestor, A. Vílchez, C. Solans, J. Esquena, Facile Synthesis of Meso/Macroporous Dual Materials with Ordered Mesopores Using Highly Concentrated Emulsions Based on a Cubic Liquid Crystal, Langmuir. 29 (2013) 432–440. https://doi.org/10.1021/la303801b.

[27] J.-L. Blin, J. Jacoby, S. Kim, M.-J. Stébé, N. Canilho, A. Pasc, A meso-macro compartmentalized bioreactor obtained through silicalization of “green” double emulsions: W/O/W and W/SLNs/W, Chem. Commun. 50 (2014) 11871–11874. https://doi.org/10.1039/C4CC06007E.

[28] M. Hoarau, S. Badieyan, E.N.G. Marsh, Immobilized enzymes: understanding enzyme – surface interactions at the molecular level, Org. Biomol. Chem. 15 (2017) 9539–9551. https://doi.org/10.1039/C7OB01880K.

[29] T. Jesionowski, J. Zdarta, B. Krajewska, Enzyme immobilization by adsorption: a review, Adsorption. 20 (2014) 801–821. https://doi.org/10.1007/s10450-014-9623-y.

[30] D.-M. Liu, J. Chen, Y.-P. Shi, Advances on methods and easy separated support materials for enzymes immobilization, TrAC Trends in Analytical Chemistry. 102 (2018) 332–342. https://doi.org/10.1016/j.trac.2018.03.011.

[31] N. Canilho, J. Jacoby, A. Pasc, C. Carteret, F. Dupire, M.J. Stébé, J.L. Blin, Isocyanate-mediated covalent immobilization of Mucor miehei lipase onto SBA-15 for transesterification reaction, Colloids and Surfaces B: Biointerfaces. 112 (2013) 139–145. https://doi.org/10.1016/j.colsurfb.2013.07.024.

[32] L. Dettori, F. Vibert, Y. Guiavarc'h, S. Delaunay, C. Humeau, J.L. Blin, I. Chevalot, N-α-acylation of lysine catalyzed by immobilized aminoacylases from Streptomyces ambofaciens in aqueous medium, Microporous and Mesoporous Materials. 267 (2018) 24–34. https://doi.org/10.1016/j.micromeso.2018.03.018.

[33] J.J. Gooding, S. Ciampi, The molecular level modification of surfaces: from self-assembled monolayers to complex molecular assemblies, Chem. Soc. Rev. 40 (2011) 2704–2718. https://doi.org/10.1039/C0CS00139B.

[34] D. Zhao, C. Peng, J. Zhou, Lipase adsorption on different nanomaterials: a multi-scale simulation study, Phys. Chem. Chem. Phys. 17 (2014) 840–850. https://doi.org/10.1039/C4CP04696J.

[35] L.-C. Sang, M.-O. Coppens, Effects of surface curvature and surface chemistry on the structure and activity of proteins adsorbed in nanopores, Phys. Chem. Chem. Phys. 13 (2011) 6689–6698. https://doi.org/10.1039/C0CP02273J.

[36] J. Grimaldi, M. Radhakrishna, S.K. Kumar, G. Belfort, Stability of Proteins on Hydrophilic Surfaces, Langmuir. 31 (2015) 1005–1010. https://doi.org/10.1021/la503865b.

[37] A. Kołodziejczak-Radzimska, J. Zdarta, T. Jesionowski, Physicochemical and catalytic properties of acylase I from aspergillus melleus immobilized on amino- and carbonyl-grafted stöber silica, Biotechnology Progress. 34 (2018) 767–777. https://doi.org/10.1002/btpr.2610.

[38] A.S. Maria Chong, X.S. Zhao, Functionalized nanoporous silicas for the immobilization of penicillin acylase, Applied Surface Science. 237 (2004) 398–404. https://doi.org/10.1016/j.apsusc.2004.06.080.

[39] G. Raffaini, F. Ganazzoli, Protein Adsorption on a Hydrophobic Surface: A Molecular Dynamics Study of Lysozyme on Graphite, Langmuir. 26 (2010) 5679–5689. https://doi.org/10.1021/la903769c.

[40] F. Felsovalyi, P. Mangiagalli, C. Bureau, S.K. Kumar, S. Banta, Reversibility of the Adsorption of Lysozyme on Silica, Langmuir. 27 (2011) 11873–11882. https://doi.org/10.1021/la202585r.

[41] M. Radhakrishna, J. Grimaldi, G. Belfort, S.K. Kumar, Stability of Proteins Inside a Hydrophobic Cavity, Langmuir. 29 (2013) 8922–8928. https://doi.org/10.1021/la4014784.

[42] J. Grimaldi, M. Radhakrishna, S.K. Kumar, G. Belfort, Stability of Proteins on Hydrophilic Surfaces, Langmuir. 31 (2015) 1005–1010. https://doi.org/10.1021/la503865b.

[43] P. Shah, N. Sridevi, A. Prabhune, V. Ramaswamy, Structural features of Penicillin acylase adsorption on APTES functionalized SBA-15, Microporous and Mesoporous Materials. 116 (2008) 157–165. https://doi.org/10.1016/j.micromeso.2008.03.030.

[44] P. Villeneuve, Lipases in lipophilization reactions, Biotechnology Advances. 25 (2007) 515–536. https://doi.org/10.1016/j.biotechadv.2007.06.001.

[45] C. Bernal, F. Guzman, A. Illanes, L. Wilson, Selective and eco-friendly synthesis of lipoaminoacid-based surfactants for food, using immobilized lipase and protease biocatalysts, Food Chemistry. 239 (2018) 189–195. https://doi.org/10.1016/j.foodchem.2017.06.105.

[46] M.C. Bourkaib, S. Delaunay, X. Framboisier, L. Hôtel, B. Aigle, C. Humeau, Y. Guiavarc'h, I. Chevalot, N-acylation of L-amino acids in aqueous media: Evaluation of the catalytic performances of Streptomyces ambofaciens aminoacylases, Enzyme and Microbial Technology. 137 (2020) 109536. https://doi.org/10.1016/j.enzmictec.2020.109536.

[47] M. Lazghab, K. Saleh, P. Guigon, Functionalisation of porous silica powders in a fluidised-bed reactor with glycidoxypropyltrimethoxysilane (GPTMS) and aminopropyltriethoxysilane (APTES), Chemical Engineering Research and Design. 88 (2010) 686–692. https://doi.org/10.1016/j.cherd.2009.11.005.

[48] O. Olkhovyk, M. Jaroniec, Periodic Mesoporous Organosilica with Large Heterocyclic Bridging Groups, J. Am. Chem. Soc. 127 (2005) 60–61. https://doi.org/10.1021/ja043941a.

[49] J.L. Blin, R. Bleta, J. Ghanbaja, M.J. Stébé, Fluorinated emulsions: Templates for the direct preparation of macroporous–mesoporous silica with a highly ordered array of large mesopores, Microporous and Mesoporous Materials. 94 (2006) 74–80. https://doi.org/10.1016/j.micromeso.2006.03.023.

[50] C. Garcia-Galan, Á. Berenguer-Murcia, R. Fernandez-Lafuente, R.C. Rodrigues, Potential of Different Enzyme Immobilization Strategies to Improve Enzyme Performance, Advanced Synthesis & Catalysis. 353 (2011) 2885–2904. https://doi.org/10.1002/adsc.201100534.

[51] K.S.W. Sing, D.H. Everett, R.A.W. Haul, L. Moscou, R.A. Pierotti, J. Rouquérol, T. Siemieniewska, Reporting Physisorption Data for Gas/Solid Systems With Special Reference to the Determination of Surface Area and Porosity, (n.d.). http://www.degruyter.com/view/IUPAC/iupac.57.0007 (accessed March 11, 2020).

[52] C. Carteret, J. Jacoby, J.L. Blin, Using factorial experimental design to optimize biocatalytic biodiesel production from Mucor Miehei Lipase immobilized onto ordered mesoporous materials, Microporous and Mesoporous Materials. 268 (2018) 39–45. https://doi.org/10.1016/j.micromeso.2018.04.004.

[53] D. Jung, C. Streb, M. Hartmann, Covalent Anchoring of Chloroperoxidase and Glucose Oxidase on the Mesoporous Molecular Sieve SBA-15, Int J Mol Sci. 11 (2010) 762–778. https://doi.org/10.3390/ijms11020762.

Figure captions

Fig 1. Nitrogen sorption isotherms (A), mesopores pore size distribution (B) and SAXS patterns (C) before and after immobilization of the non-functionalized SBA-15 (1) and MMS (2)

Fig 2. Pore size distribution obtained by mercury porosity analysis (1) and scanning electron microscopy images of MMS (2)

Fig 3. Relative activity of the immobilized acylases after support recycling compared to the initial activity set at 100%. in blue: relative conversion of the alpha acetyl-lysine, in red: relative conversion of the alpha acetyl-lysine reported by the amount of the protein present in the reaction medium

Fig 4. ^{29}Si CPMAS NMR spectra (a) and ^{13}C CPMAS NMR spectra (b) of SBA-15 (1) and MMS (2) materials with and without acylases.,

Fig 5. SAXS patterns of the silica materials without (a, c, e, g, i, k) and with enzyme (b, d, f, h, j, l). Non-functionalized (a, b) and functionalized (c, d, e, f, g, h, I, j, k, l) SBA-15 (A) and MMS (B) have been used. Nitrogen sorption isotherms of SBA-15 (C) and MMS (D) functionalized with 0 (a), 11 (b), 5 (c) and 50 % (d) of APTES.

Fig 6. Specific surface area (A), porous volume (B) and pore diameter (C) evolution after functionalization and immobilization steps on MMS and SBA-15 supports and evolution of the porous volume of the 5% and 50% APTES functionalized MMS and SBA-15 supports after treatment with the buffer used for the immobilization with and without enzyme (D).

Fig 7. Amount of enzymes adsorbed on functionalized SBA-15 and MMS materials after 18 h immobilization at 4°C under 100 rpm rotatory agitation.

Fig 8. A. Determination of the N-α-acetyl-L-lysine hydrolytic activity of both APTES functionalized materials (24 h at 37 °C, 500 rpm), B. relative residual adsorbed proteins on the APTES functionalized SBA15 after re-use for 3 cycles, C. relative synthetic activity compared to the free enzymes (72 h at 45°C, 600 rpm), D. relative hydrolytic activity of the cross-linked enzyme aggregate post immobilization on the SBA15 functionalized with 50% APTES (24 h at 37 °C, 500 rpm)

Figures:

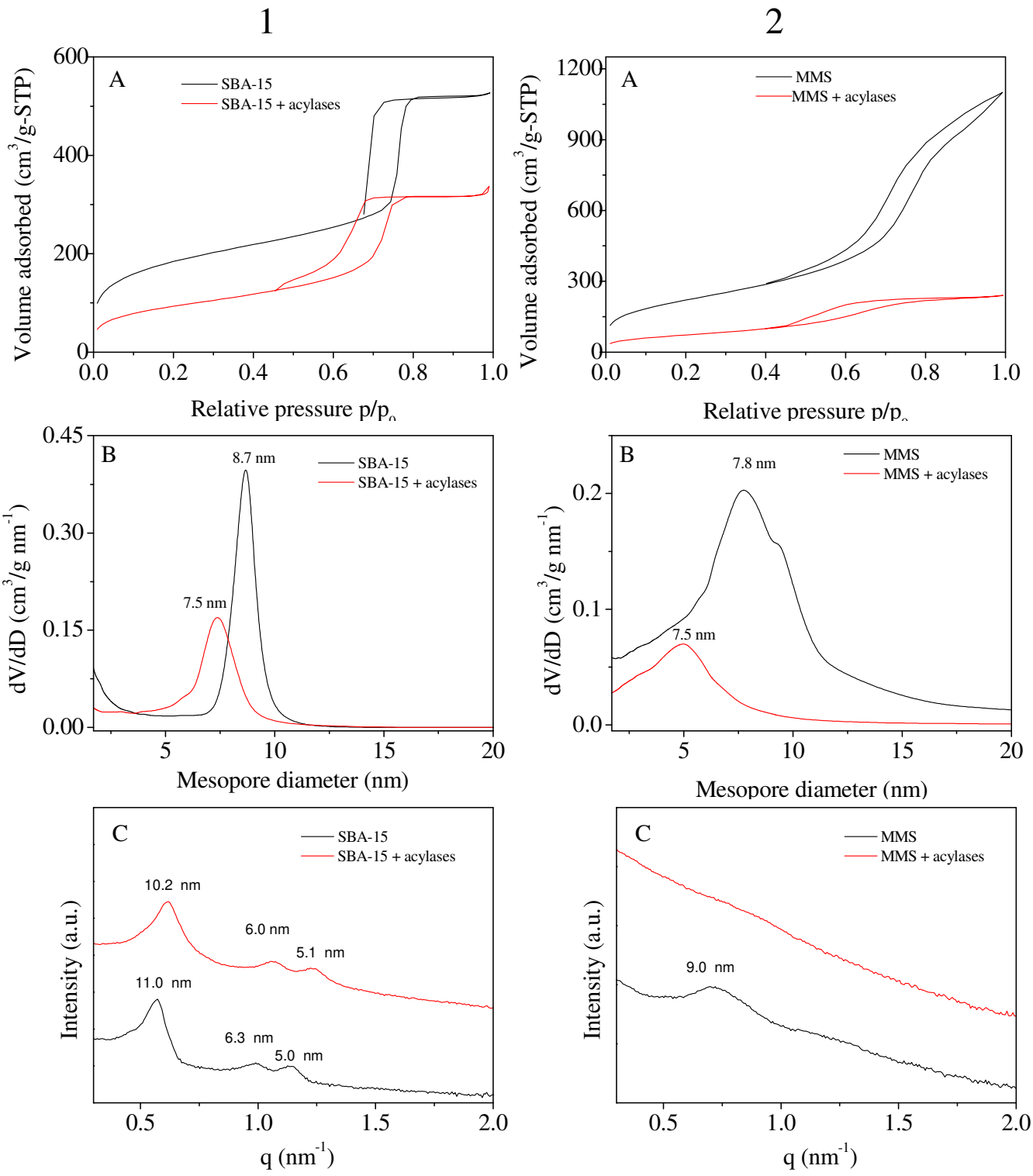

Fig 1.

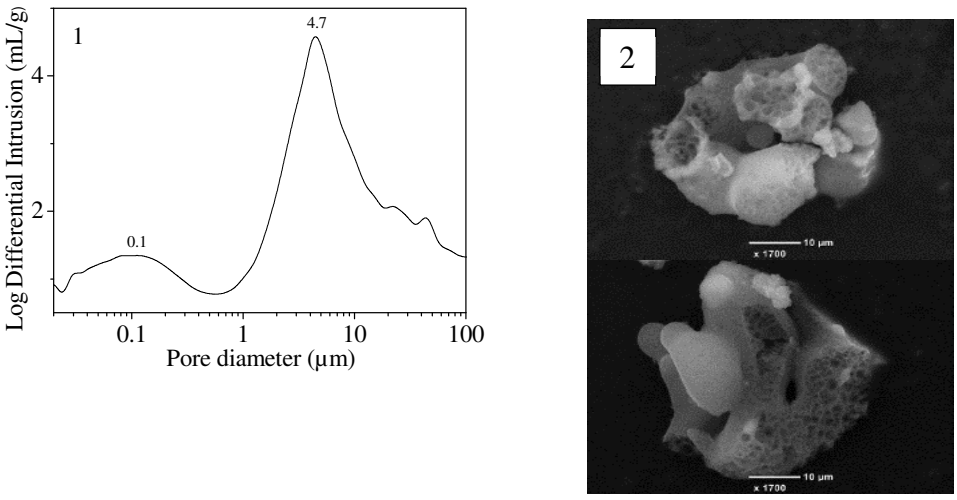
1
4.7
0.1
Log Differential Intrusion (mL/g)
4
2
0.1
1
10
100
Pore diameter (µm)
2
10 µm
x 1700
10 µm
x 1700

Fig 2.

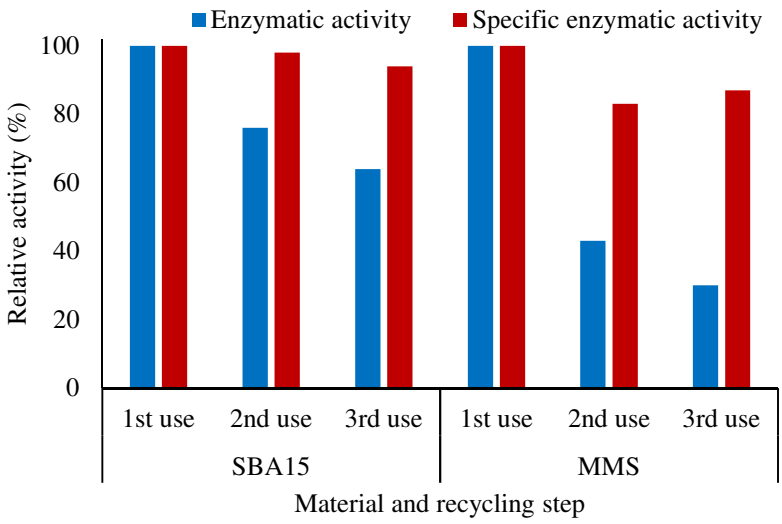
Enzymatic activity
Specific enzymatic activity
Relative activity (%)
100
80
60
40
20
0
1st use
2nd use
3rd use
1st use
2nd use
3rd use
SBA15
MMS
Material and recycling step

Fig 3.

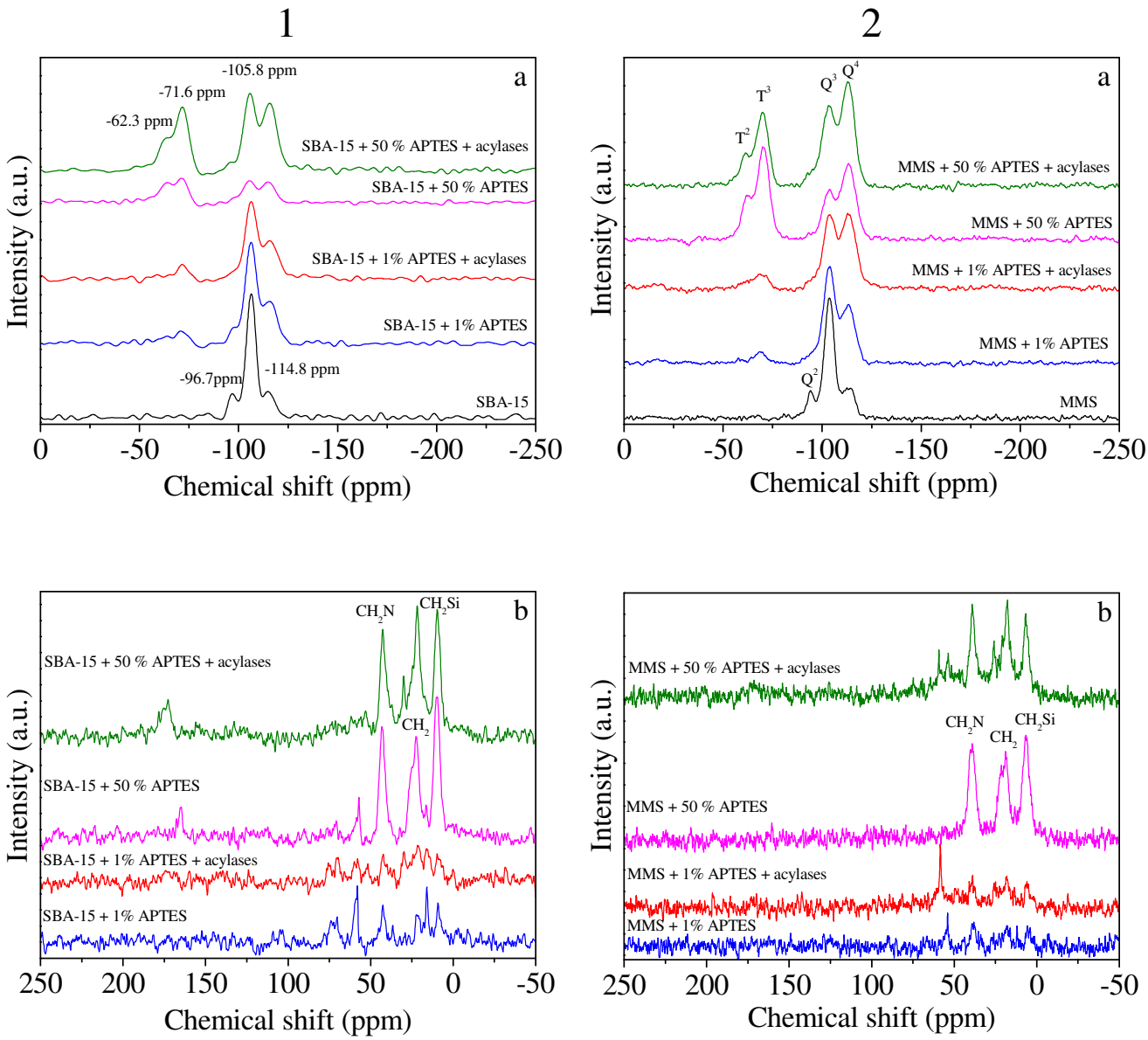
1
2
a
b
-105.8 ppm
-71.6 ppm
-62.3 ppm
-96.7ppm
-114.8 ppm
SBA-15 + 50 % APTES + acylases
SBA-15 + 50 % APTES
SBA-15 + 1% APTES + acylases
SBA-15 + 1% APTES
SBA-15
MMS + 50 % APTES + acylases
MMS + 50 % APTES
MMS + 1% APTES + acylases
MMS + 1% APTES
MMS
T2
T3
Q3
Q4
Q2
CH2N
CH2Si
CH2
Intensity (a.u.)
Chemical shift (ppm)

Fig 4.

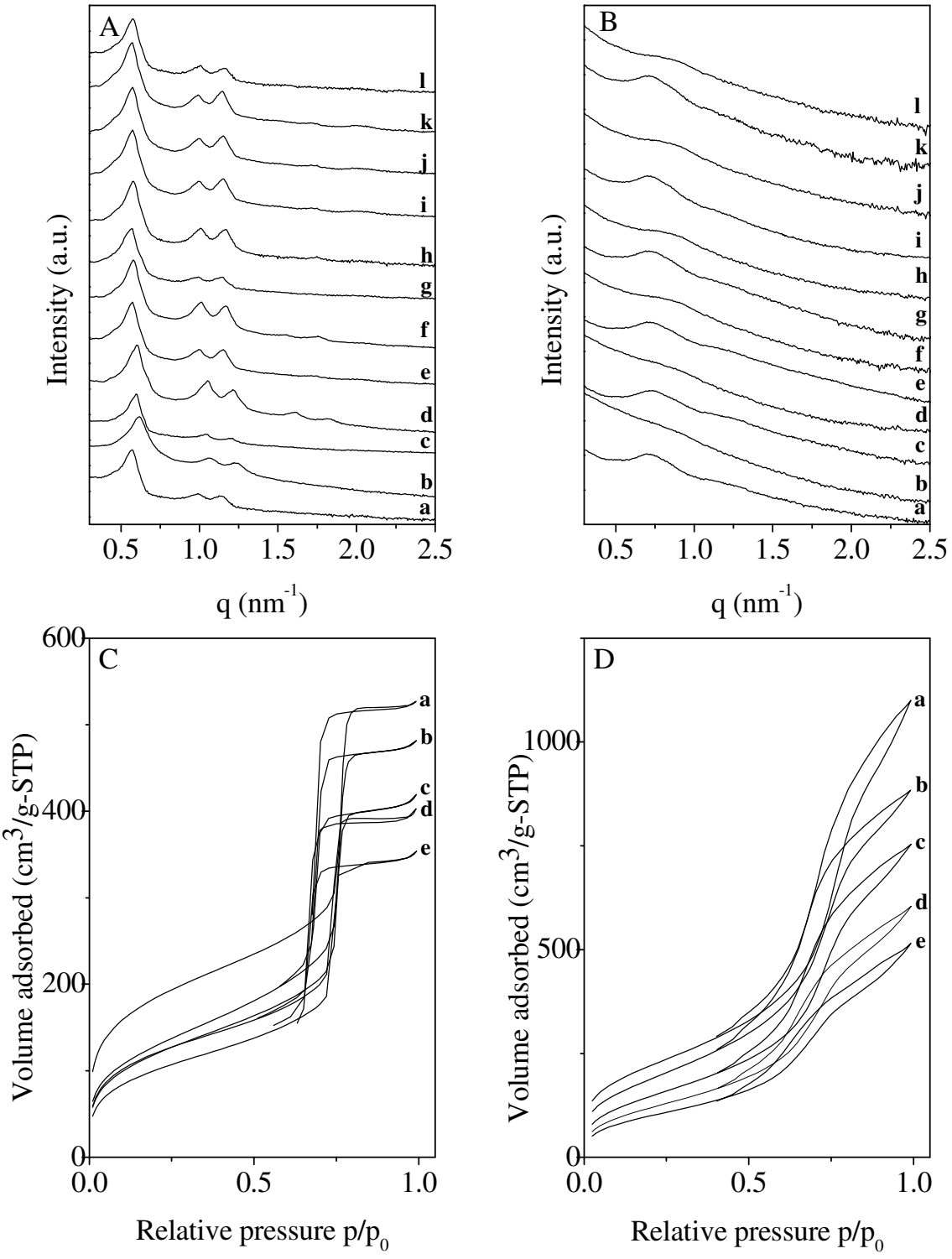
A
B
C
D
Intensity (a.u.)
q (nm^{-1})
Volume adsorbed (cm^3/g-STP)
Relative pressure p/p$_0$
a
b
c
d
e
f
g
h
i
j
k
l

Fig 5.

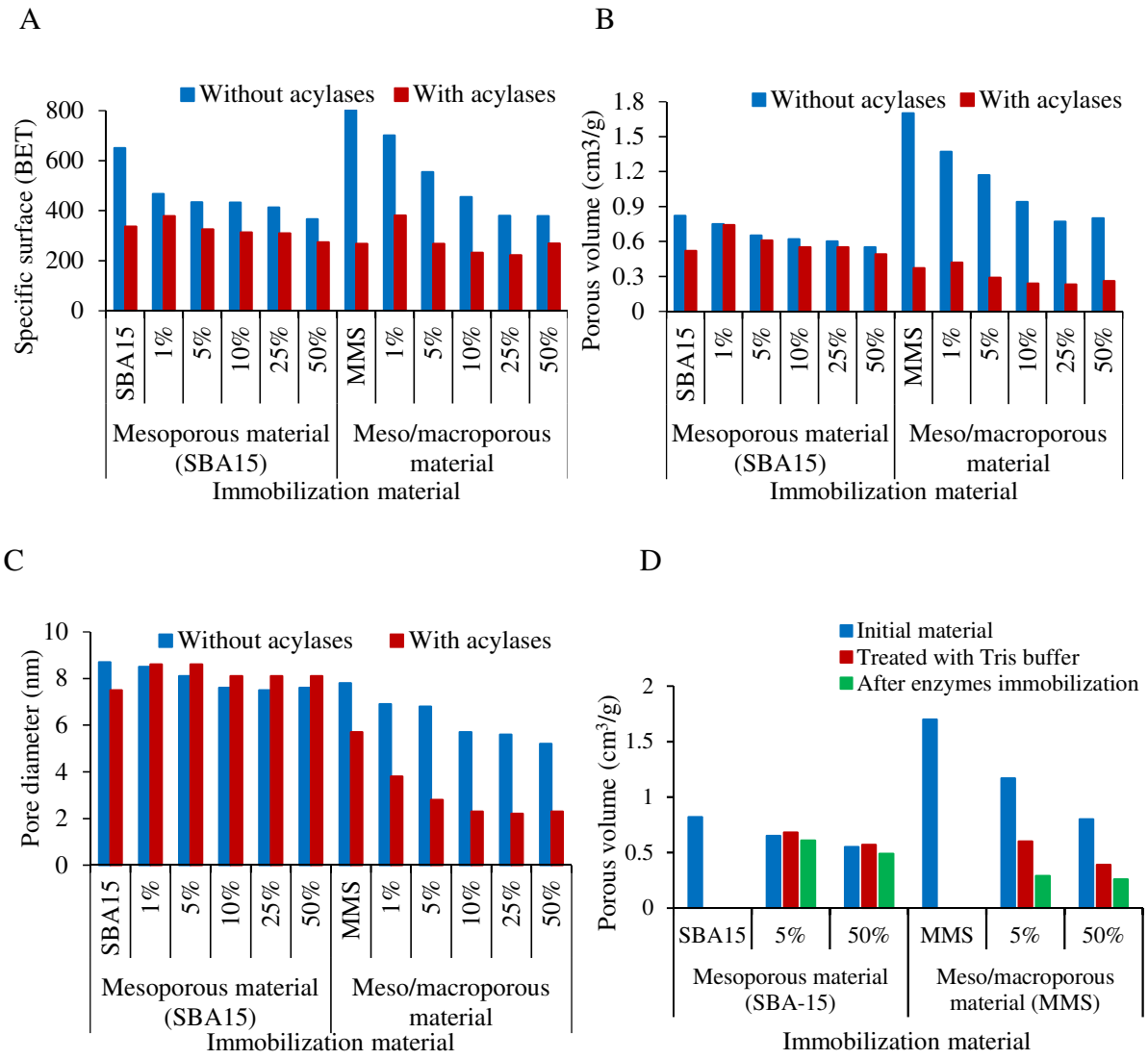
A
Without acylases
With acylases
Specific surface (BET)
800
600
400
200
0
SBA15
1%
5%
10%
25%
50%
MMS
1%
5%
10%
25%
50%
Mesoporous material (SBA15)
Meso/macroporous material
Immobilization material
B
Without acylases
With acylases
Porous volume (cm3/g)
1.8
1.5
1.2
0.9
0.6
0.3
0
SBA15
1%
5%
10%
25%
50%
MMS
1%
5%
10%
25%
50%
Mesoporous material (SBA15)
Meso/macroporous material
Immobilization material
C
Without acylases
With acylases
Pore diameter (nm)
10
8
6
4
2
0
SBA15
1%
5%
10%
25%
50%
MMS
1%
5%
10%
25%
50%
Mesoporous material (SBA15)
Meso/macroporous material
Immobilization material
D
Initial material
Treated with Tris buffer
After enzymes immobilization
Porous volume (cm3/g)
2
1.5
1
0.5
0
SBA15
5%
50%
MMS
5%
50%
Mesoporous material (SBA-15)
Meso/macroporous material (MMS)
Immobilization material

Fig 6.

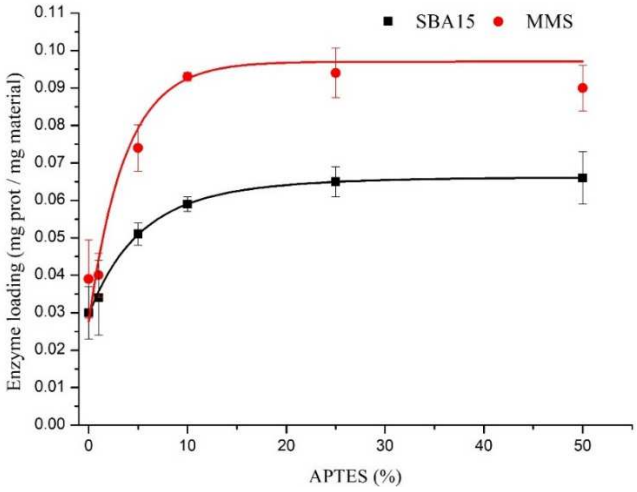
SBA15
MMS
Enzyme loading (mg prot / mg material)
APTES (%)
0.11
0.10
0.09
0.08
0.07
0.06
0.05
0.04
0.03
0.02
0.01
0.00
0
10
20
30
40
50

Fig 7.

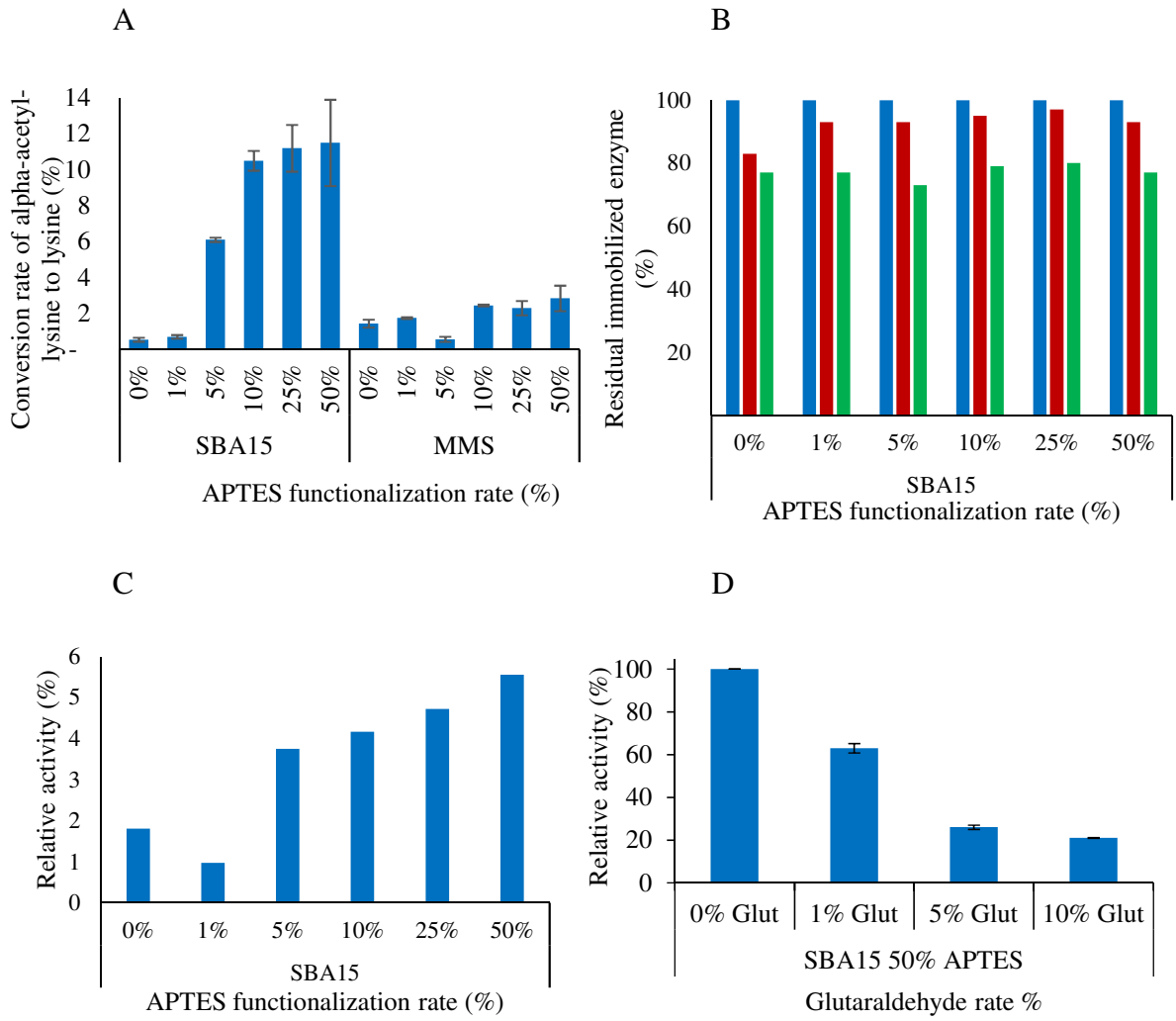
A
Conversion rate of alpha-acetyl-lysine to lysine (%)
14
12
10
8
6
4
2
-
0%
1%
5%
10%
25%
50%
0%
1%
5%
10%
25%
50%
SBA15
MMS
APTES functionalization rate (%)
B
Residual immobilized enzyme (%)
100
80
60
40
20
0%
1%
5%
10%
25%
50%
SBA15
APTES functionalization rate (%)
C
Relative activity (%)
6
5
4
3
2
1
0
0%
1%
5%
10%
25%
50%
SBA15
APTES functionalization rate (%)
D
Relative activity (%)
100
80
60
40
20
0
0% Glut
1% Glut
5% Glut
10% Glut
SBA15 50% APTES
Glutaraldehyde rate %

Fig 8.

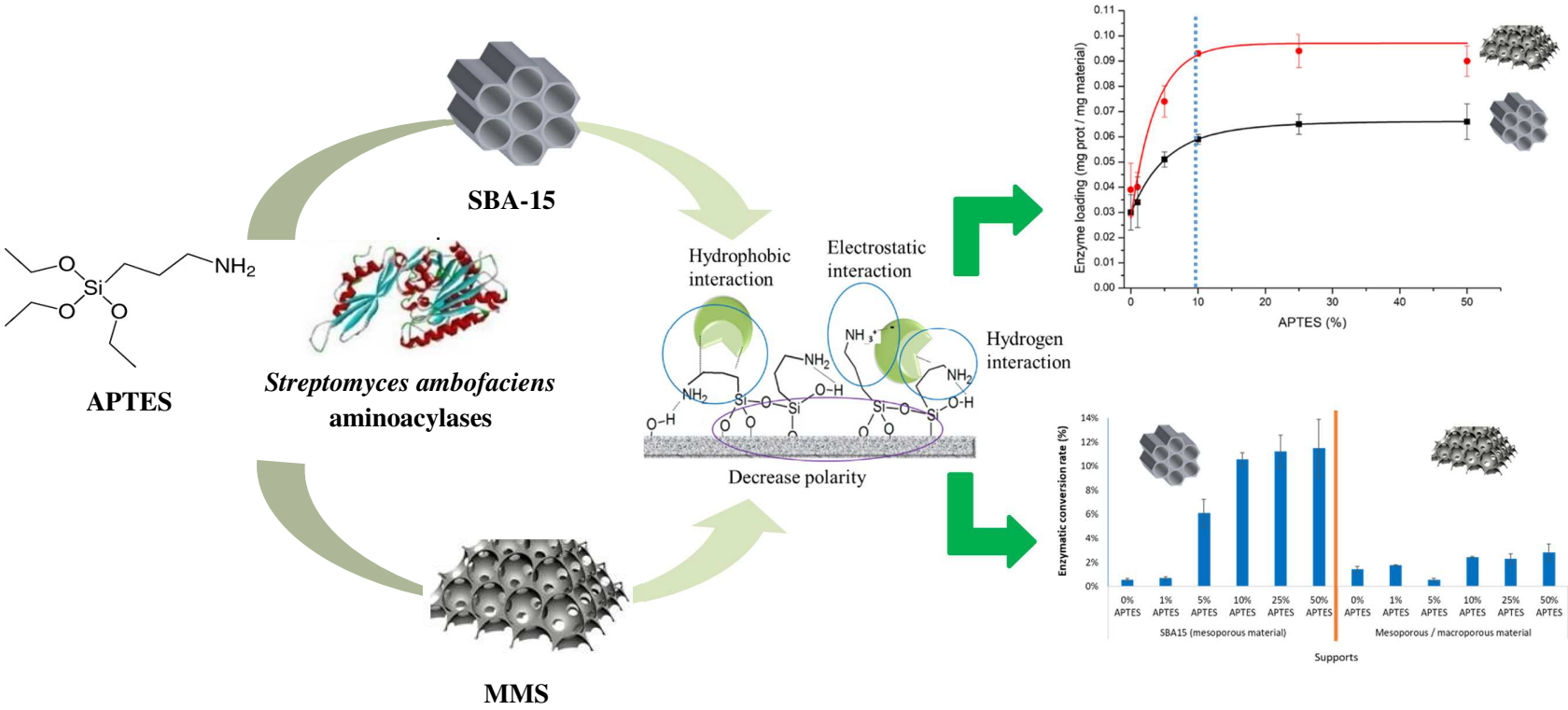
SBA-15
APTES
Streptomyces ambofaciens
aminoacylases
MMS
Hydrophobic interaction
Electrostatic interaction
Hydrogen interaction
Decrease polarity
Enzyme loading (mg prot / mg material)
APTES (%)
Enzymatic conversion rate (%)
0% APTES
1% APTES
5% APTES
10% APTES
25% APTES
50% APTES
SBA15 (mesoporous material)
Mesoporous / macroporous material
Supports